SURFIN

Cleveland

Ohio
4th to 6th June, 2018

Session 5
Light Materials:
Treatments optimizing performance

Huntington Convention Center

“Nanoporous anodic oxides: Fabrication, applications, sensing and biosensing“

Xavier Albort Ventura, Ph.D.,

Laboratory Electrochemical R & D Barcelona, Spain
University Politecnic of Catalunya, Barcelona, Spain
Tecnocrom Industrial Cabrera de Mar –Barcelona, Spain

ABSTRACT

- Numerous metals are subjected to the anodic oxidation. As a results one can obtain amorphous barrier-type oxide,crystalline barrier-type oxide or amorphous nanoporous oxide

- Currently highly-ordered nanoporous anodic aluminium oxide(AAO),is obtained with various electrolytes to form nanostructures with a wide range of geometrical features, it allows applications for this material as a template for nanofabrication of variety of nanowires, nanotubes and nanodots

- Also other anodic oxides attract attention of the researches for example anodic titania is currently applied as a key material in dye sensitized solar cells (DSSC).
- Anodic titania was found to be also an efficient catalyst for water splitting and carbon dioxide removal additional, anodic zirconia nanotubes serve as efficient support for surface Enhanced Raman Spectroscopy

Nanoporous anodic alumina (NAA).The ordered pores import with unique optical and electrochemical properties ,this chapter provides detailed fundamental of sensing techniques and recent advances in development of NAA based sensing and biosensing technologies .

Key words:

- Nanostructures porous alumina AAO membranes
- Porous Alumina AAO membranes are widely used for fabrication of various nanostructures and nano-devices
- Porous Alumina excellent structures
- Nanopourus anodic alumina NAA

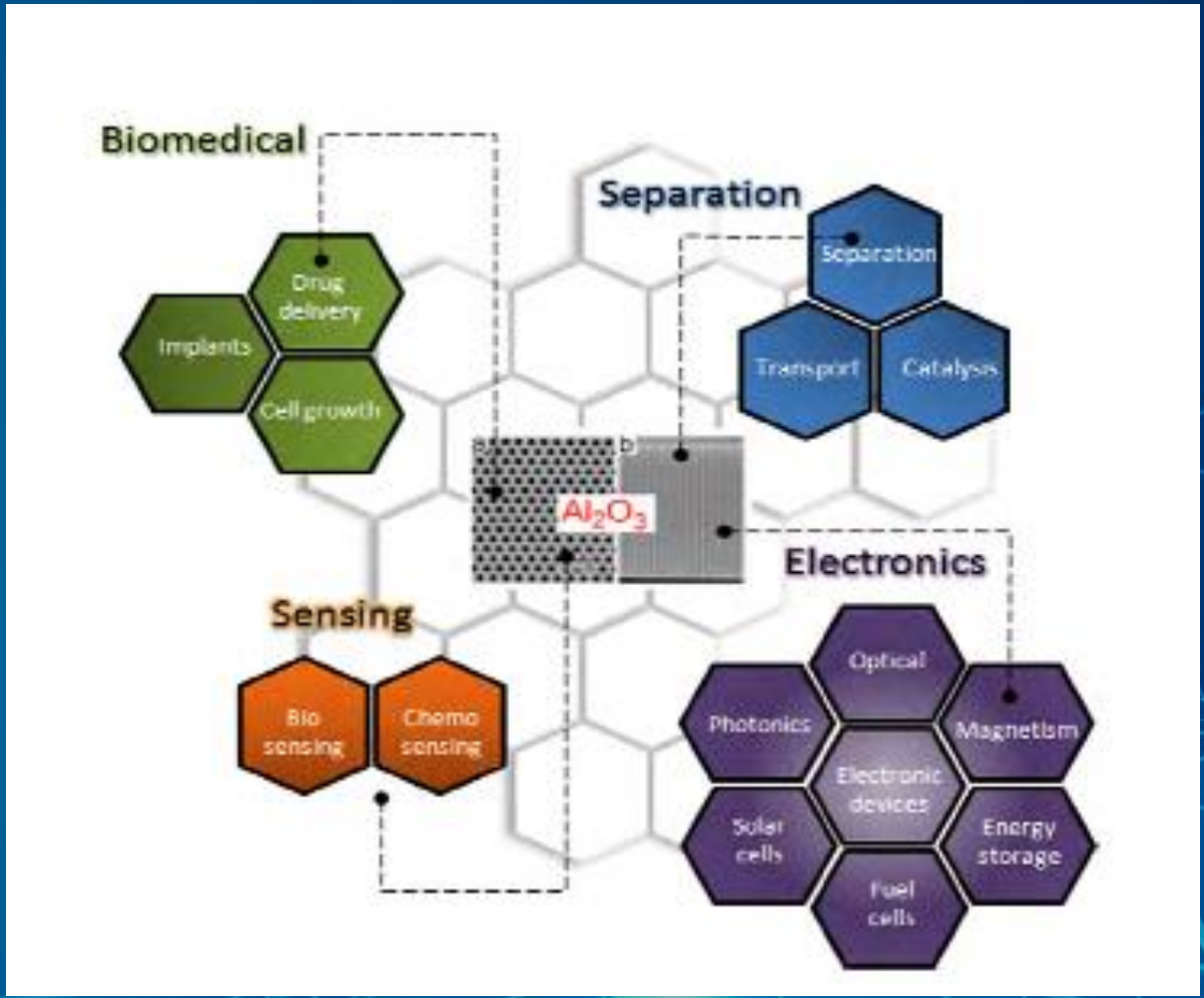

Fig. 1. Scheme showing the typical AAO structure and the major applications for this nanostructured material.

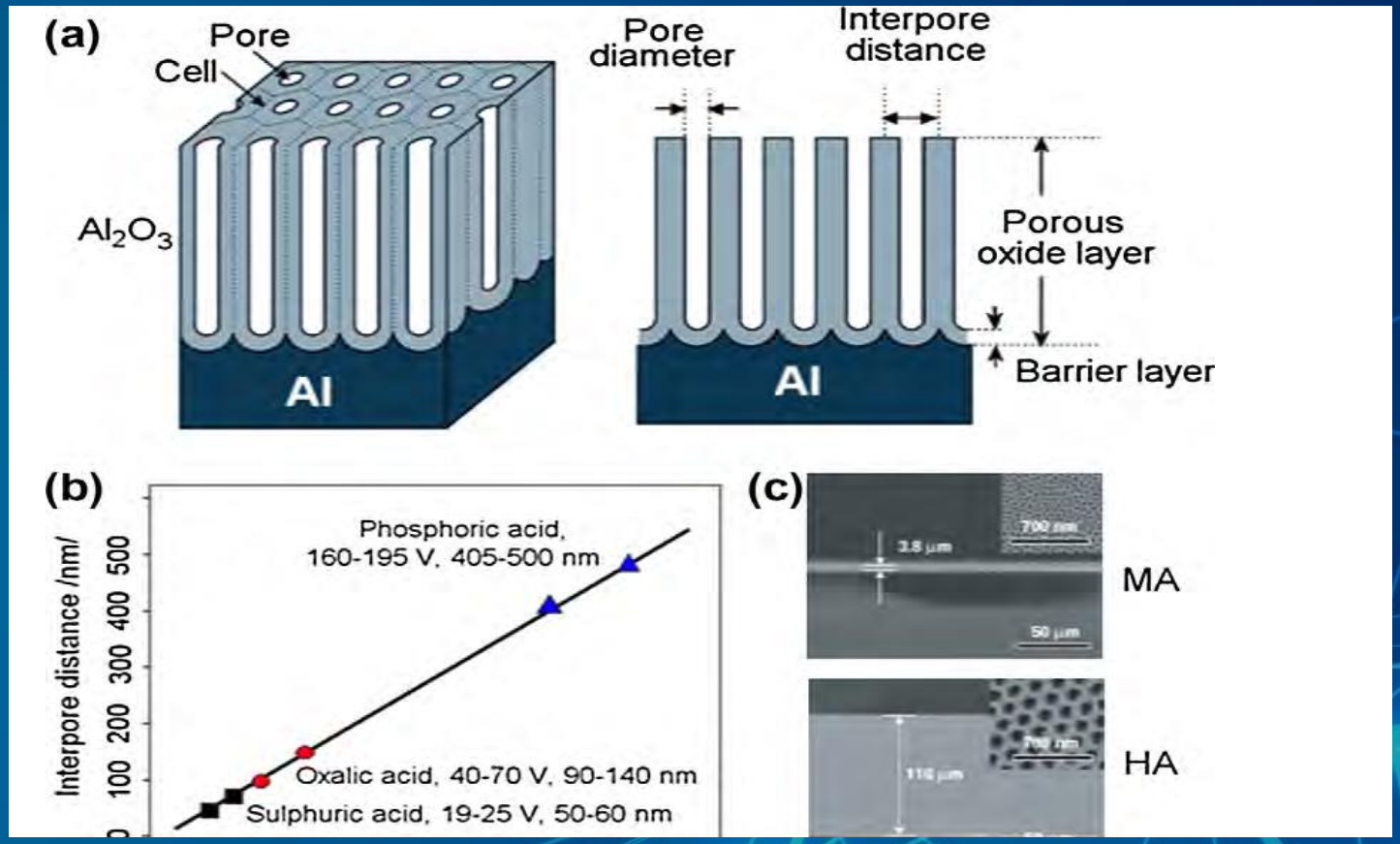

Fig. 2. (a) Schematic drawing of AAO structure prepared by electrochemical anodization of Al. (b) Summary of self-ordering voltage and corresponding interpore distance of AAO produced within three well-known regimes of electrolytes (sulfuric, oxalic and phosphoric). (c) (Top) SEM cross-sectional view of AAO membrane formed by MA (0.3 M H2C2O4, 1 °C, 40 V) and (bottom) by HA (at 140 V) for 2 h (insets: SEM top view of pore structures).

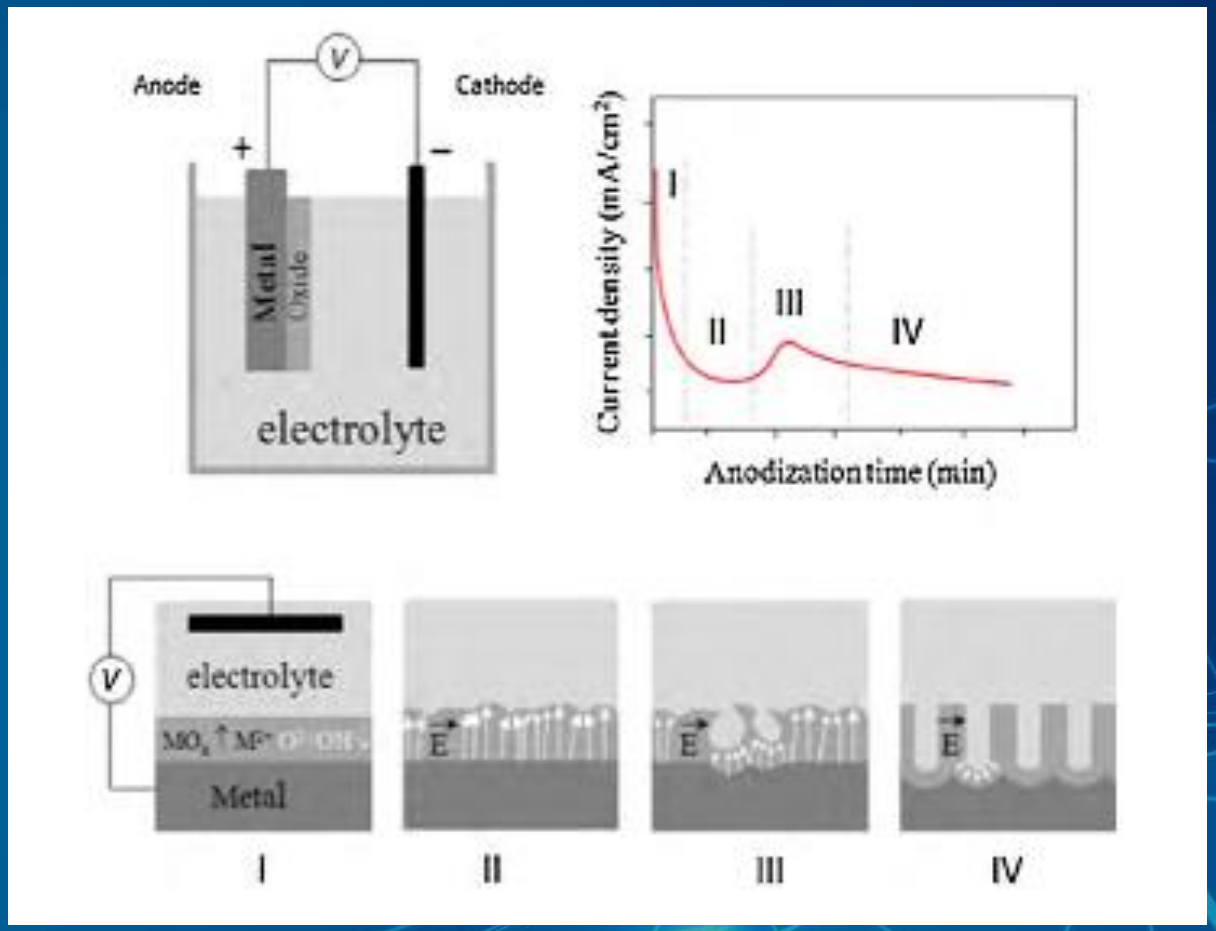

Fig. 3. Schematic diagram of the self ordering process of pore formation by electrochemical anodization including electrochemical cell set-up and typical current density curve of electrochemical anodization. Stages of pore growth: (I) formation of oxide layer; (II) formation of pits by local electric field heterogeneities; (III) initial pore formation; (IV) pore growth under steady-state conditions

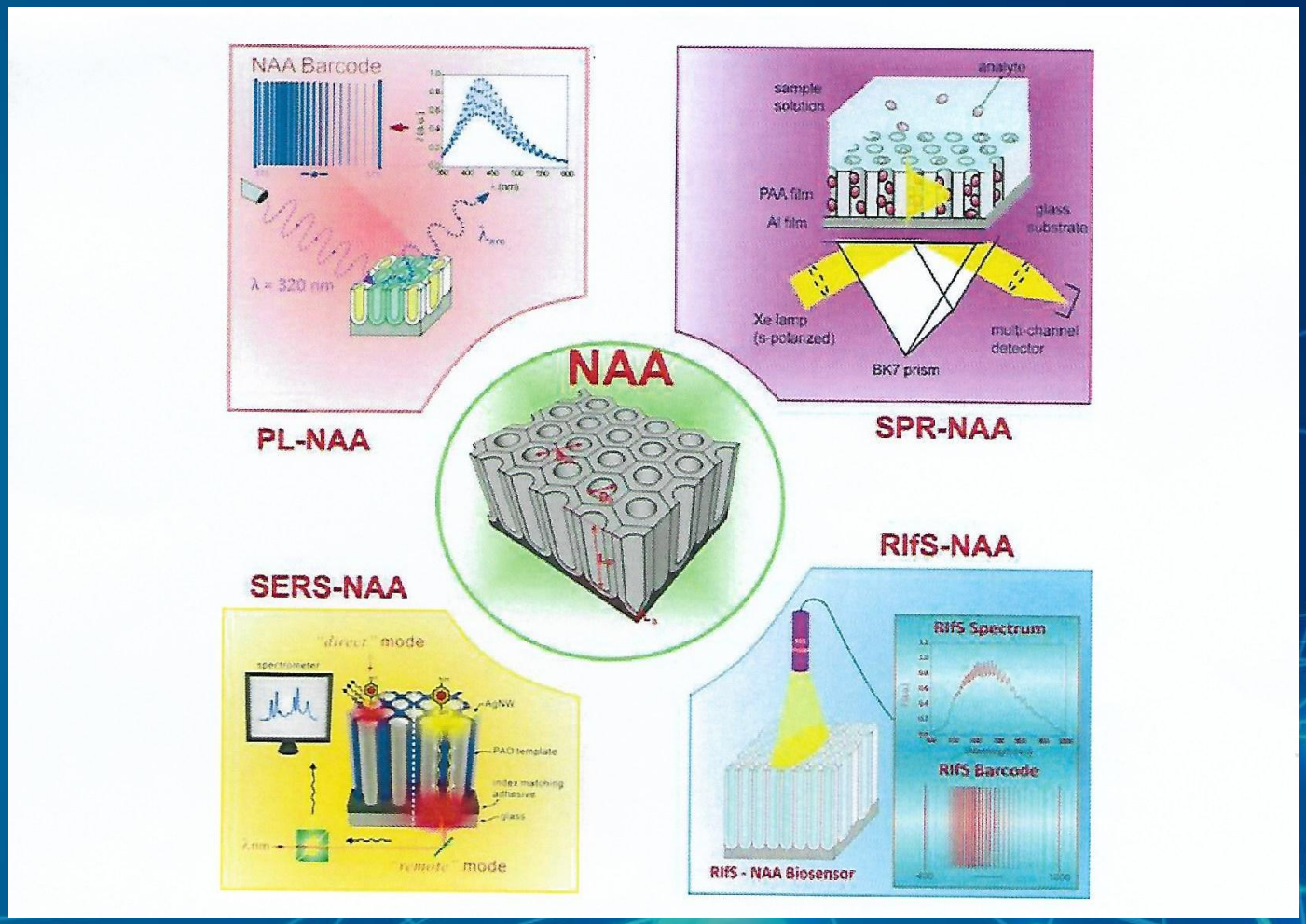

Fig. 4. A schemating showing all four optical sensing techniques coupled with NAA for developing highly sensitive optical sensors

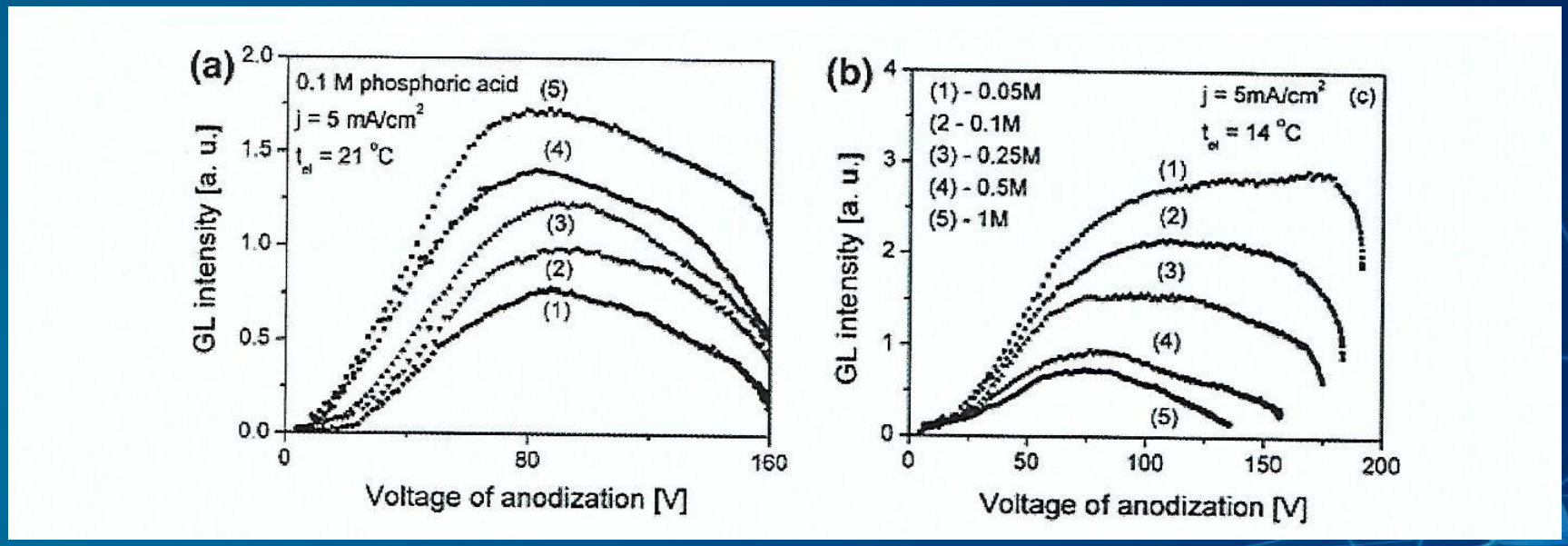

Fig. 5. GL intensity plots for NAA displaying intensity of GL against voltage for (**a**) different annealing temperature (1) 75°C; (2) 150°C; (3) 250°C; (4) 350°C; (5) 450°C; and (**b**) varying electrolyte concentrations

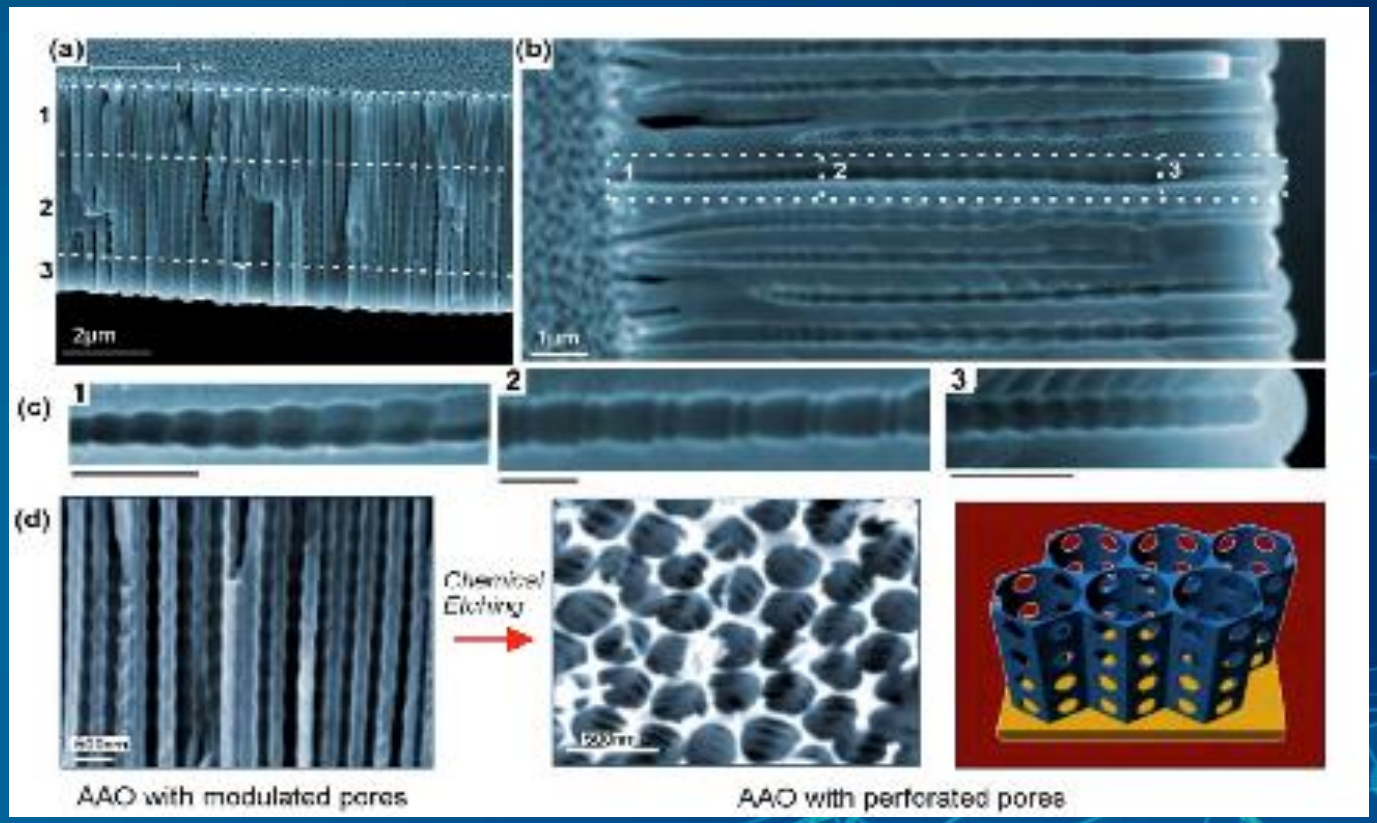

Fig. 6 (Top): (a–c) SEM image of AAO with multilayered pore architectures with different pore shapes and structural modulation fabricated by multiple cyclic anodization in 0.1 M phosphoric acid with three successive galvanostatic anodization steps by three different cyclic signals. (d) AAO with periodically perforated pores (nanopores with nanoholes) by chemical etching. Adapted with permission from Ref. [78].

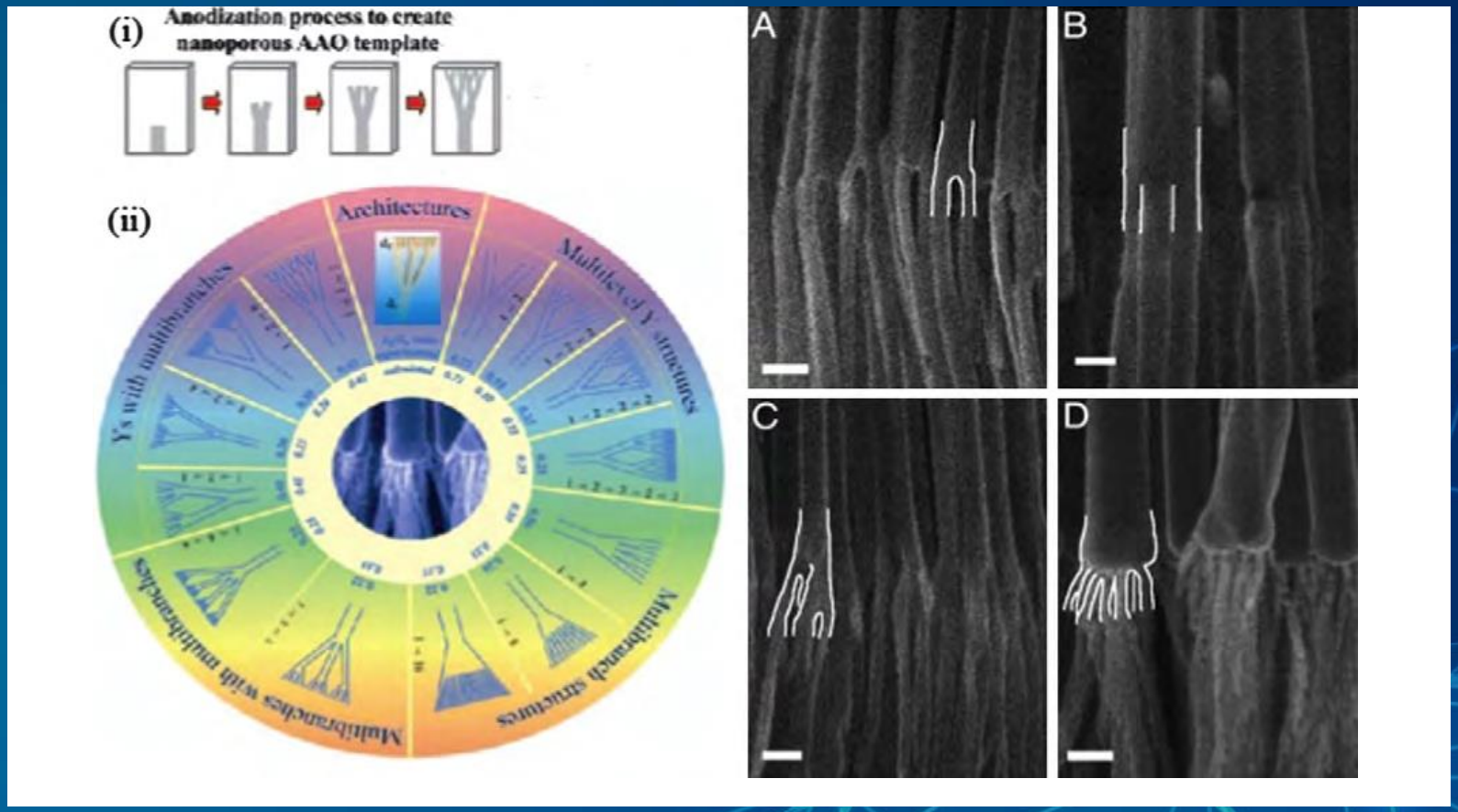

Fig. 7. (Left): (i) Schematic showing the fabrication process, where pores with controlled architectures are developed by consecutive steps of anodization and then used as molds to cast nanotubes and nanowires of complex geometries. (ii) Schematic showing a catalogue of pore architectures categorized in the schematic based on four different hierarchies of branching of stems: multiple generations of Y-branching from one stem, multiple branching from individual stems, combination of Y-branching with each branch undergoing multiple-branching (or reverse), and a combination of multiple branching with each branch developing multiple branches. (Right): Series of SEM images of multiply branched structures of carbon nanotubes (CNT) confirming branched structure of the AAO template. The primary stem branches into 2 (A), 3 (B), 4 (C), and 16 (D) pores, respectively. The junctions are highlighted with white line contours for clarity. Adapted with permission from Ref. [69].

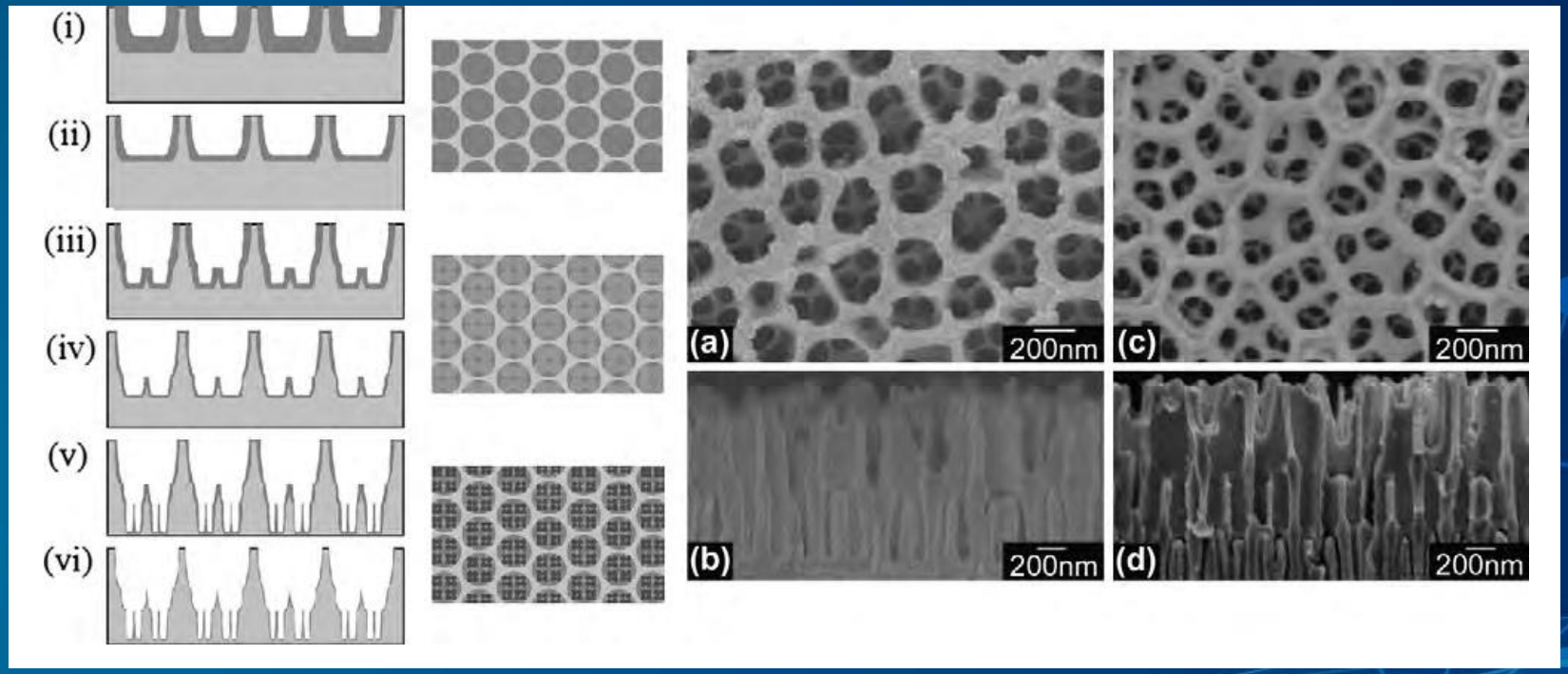

Fig. 8. (Left): Schematic of the sequential fabrication steps of three-tiered branched AAO. (i and ii) First step, first-tier pore anodization and thinning of barrier layer. (iii and iv) Second step, second tier formation at reduced potential followed by thinning of barrier layer. (v and vi) Third step, formation of third-tiered pores at further reduced anodization potential and final pore widening and (middle) corresponding top views of all tiers. (Right): SEM microscopy of the resulting pore structures. (a and b) Top and cross-sectional views of a two-tiered branched AAO prepared by combined anodization in 0.3 M phosphoric acid (130 V) and 0.15 M oxalic acid (80 V) followed by thinning of the barrier layer. (c and d) Top and cross-sectional views of the three-tiered branched AAO prepared by combined anodization in 0.3 M phosphoric acid (130 V), 0.15 M oxalic acid (80 V) and 0.15 M oxalic acid (80 V) followed by thinning of the barrier layer. Adapted with permission from Ref. [70].

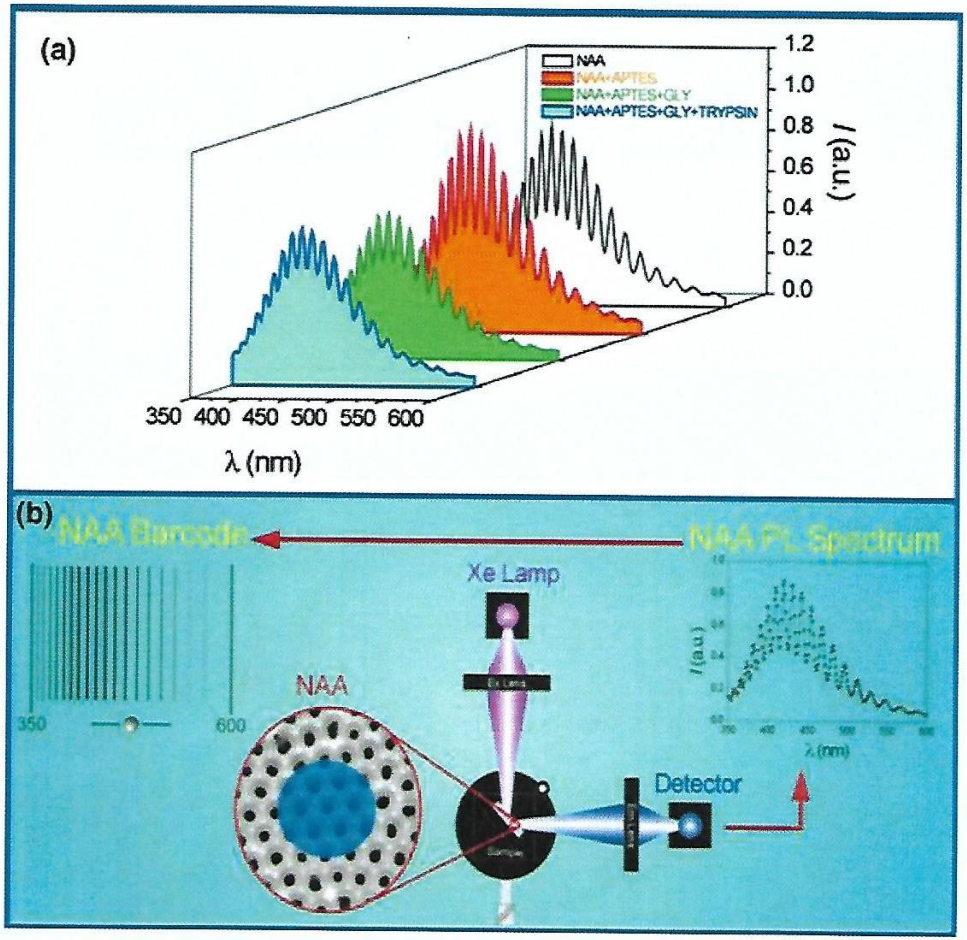

Fig. 9. (**a**) PL spectrum of NAA showing Fabry-Pérot fringes and step-wise changes in PL on attachment of trypsin side the pores. (**b**) Typical PL setup used for recording luminiscence of NAA substrate along with the FP fringes that can be converted to PL

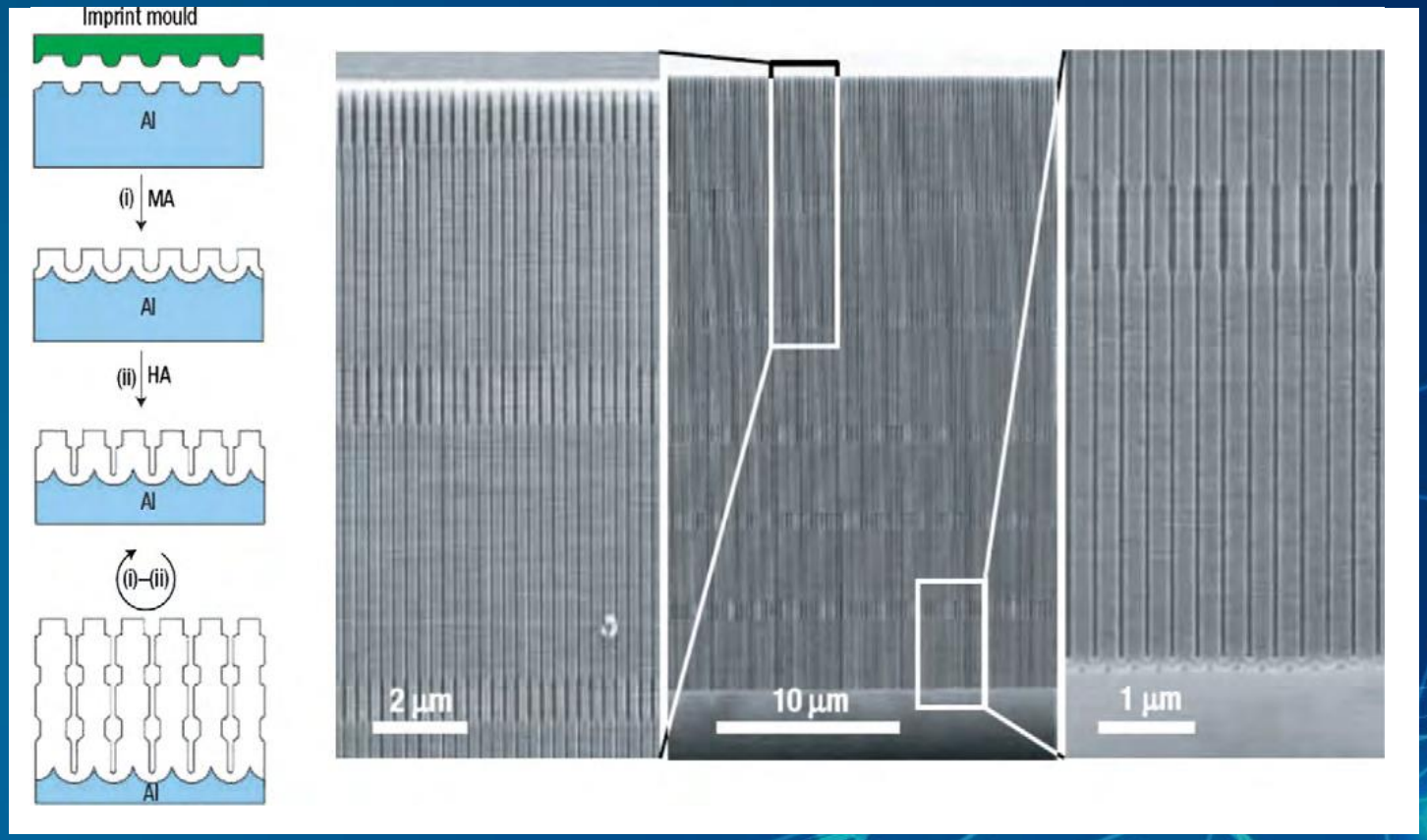

Fig. 10. Long-range ordered AAO membranes with modulated pore diameters. (Left): Scheme for the fabrication of porous alumina with modulated pore diameters by a combination of MA and HA on a pre-patterned aluminium substrate. (Right): SEM micrographs showing the cross-section of the prepared AAO with modulated pore diameters. Magnified cross-section images of the top and bottom parts of the membrane are shown on both sides of the central image. Adapted with permission from Ref. [41].

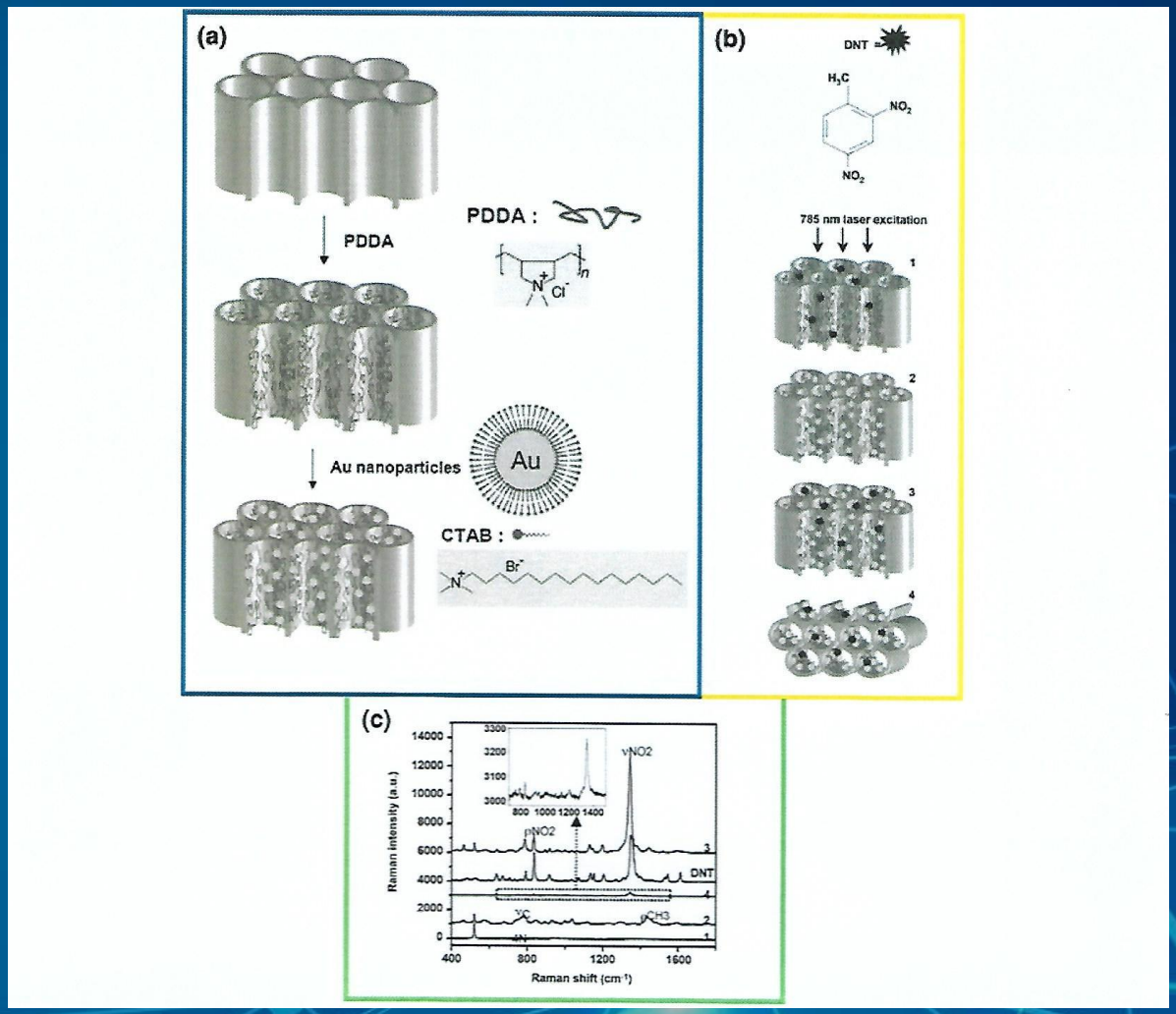

Fig. 11. Schematic demonstrating procedure of (**a**) decorating NAA with AuNPs. (**b**) Chemical structure of 2,4-DNT and schematic of Raman measurement of 2,4-DNT with different laser excitation angles parallel (1,2,3) and perpendicular (4) to the pore axes and (**c**) the Raman spectrum of DNT powder and 1000 ppm 2,4-DNT on each substrate shown schematically in (**b**)

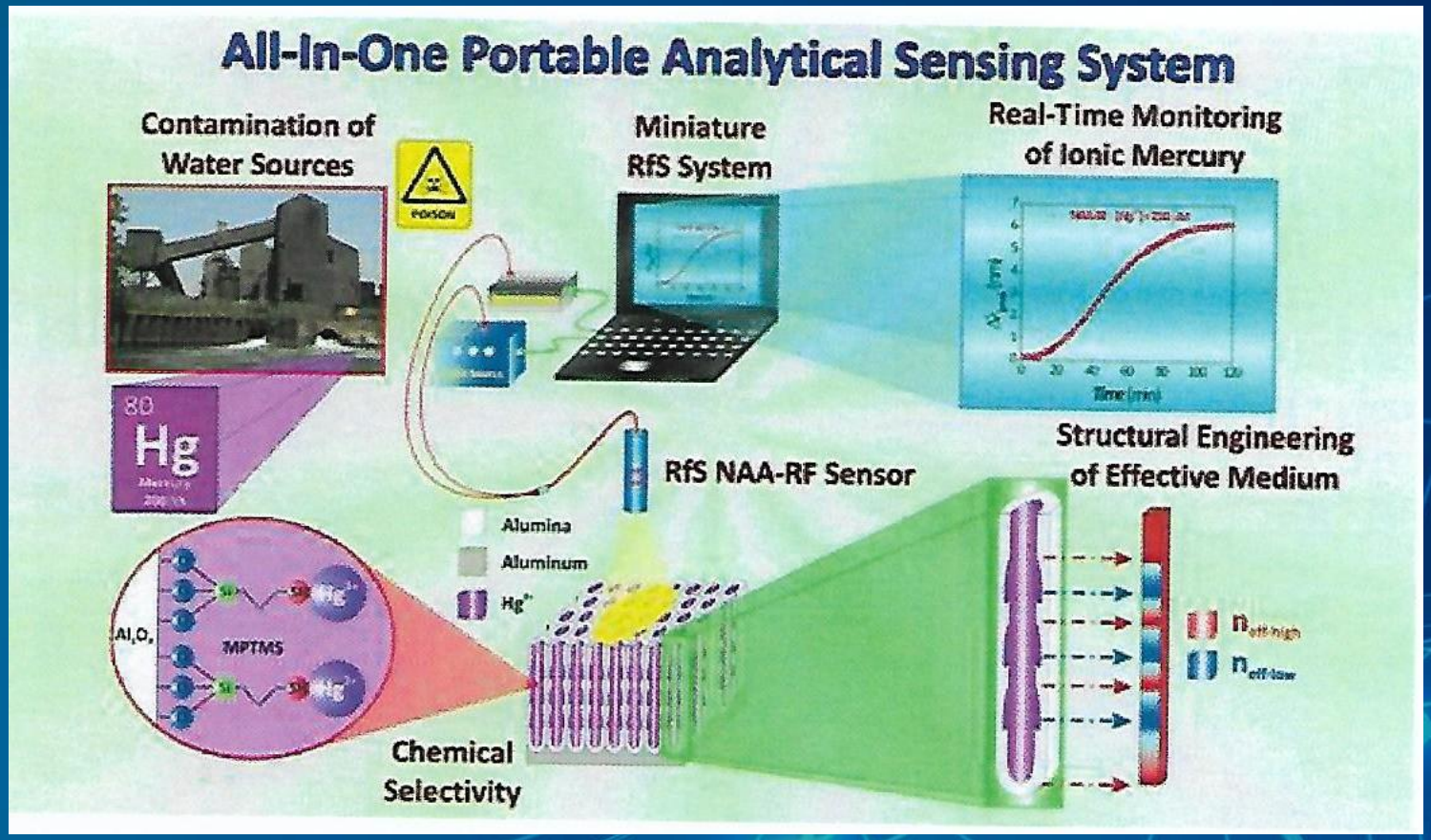

Fig. 12. A schematic describing NAA-RF based portable mercury ion sensing platform

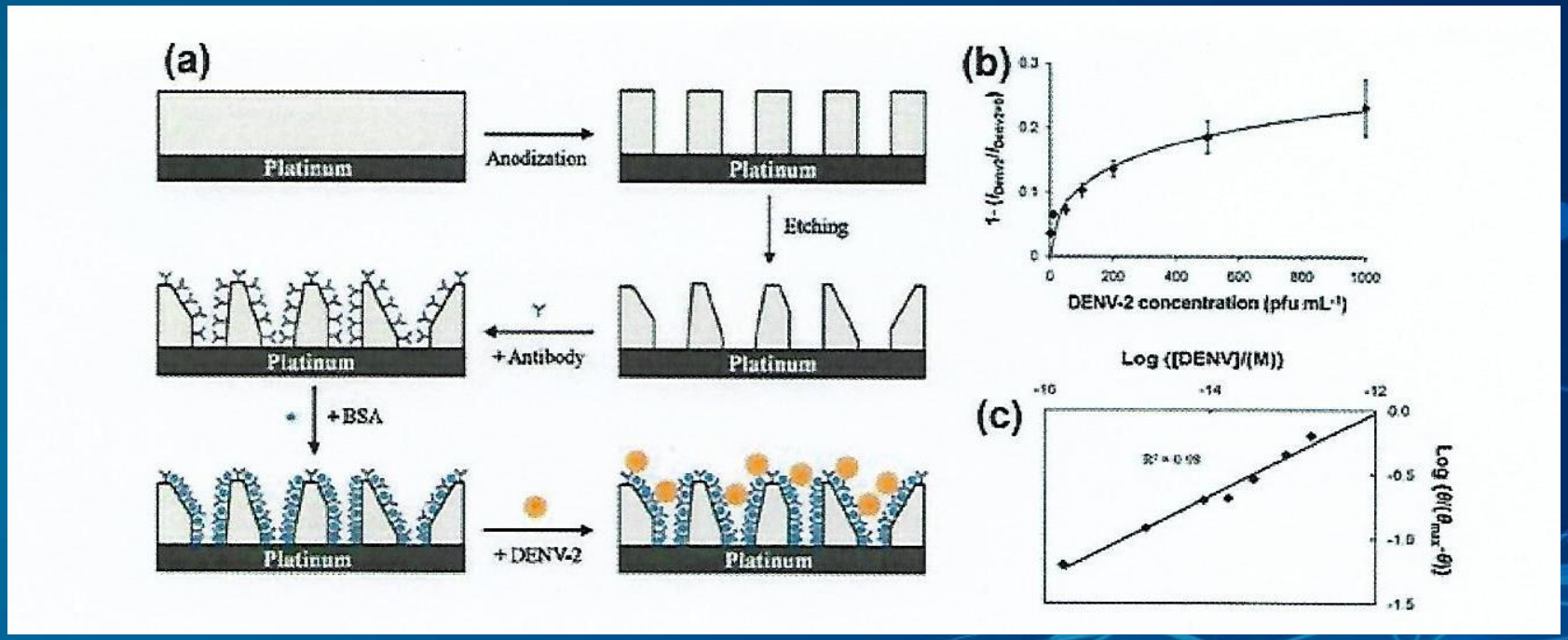

Fig. 13. (**a**) Design of NAA based electrochemical nanobiosensor for detection of DENV-2 Dengue virus. (**b**) NAA nanosensor's response toward different concentrations of DENV-2 in 0,1M phosphate and (**c**) its corresponding linear calibration curve in long values.

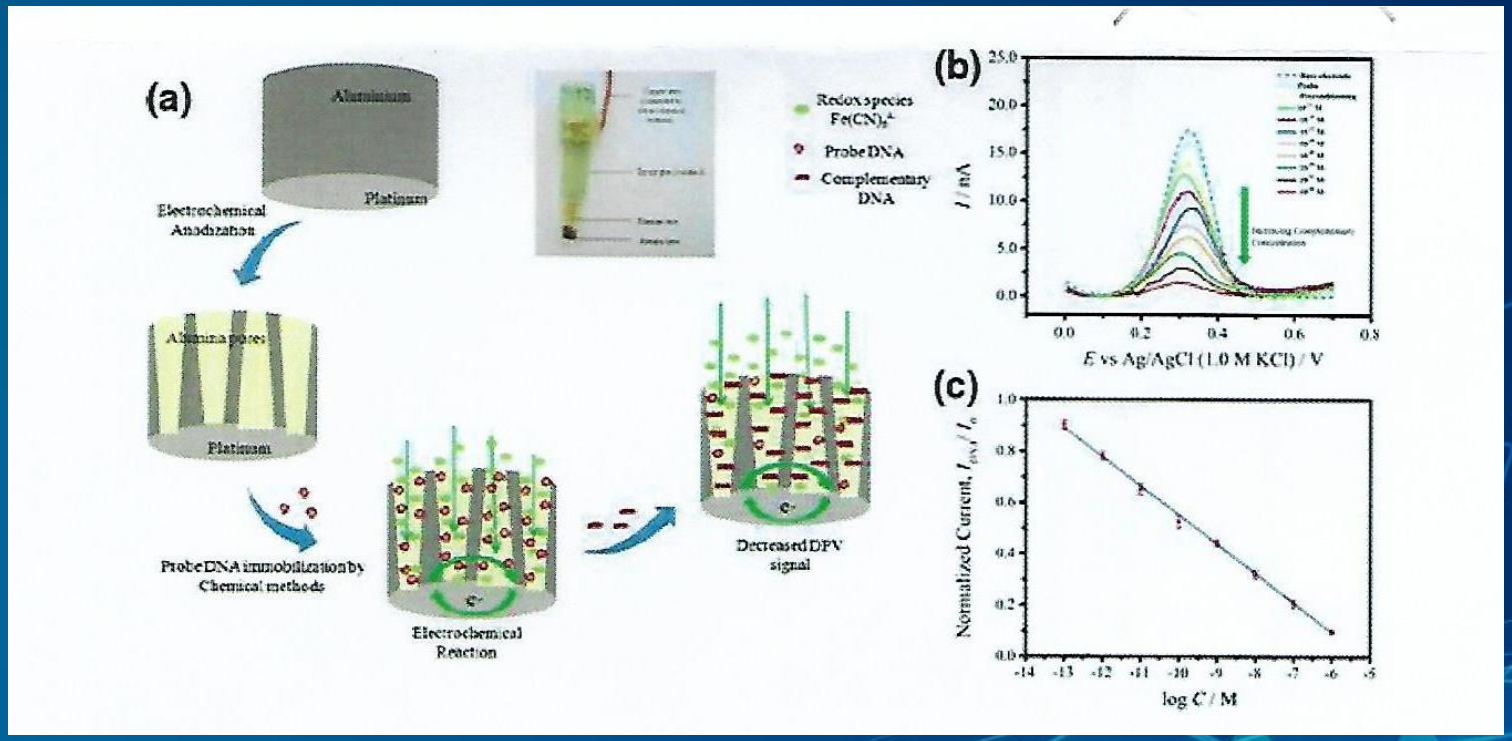

Fig. 14. (**a**) Scheme of construction of NAA based electrochemical DNA sensors. (**b**) Current signal response of bare electrode toward increasing concentration of complementary target and (**c**) its corresponding calibration curve

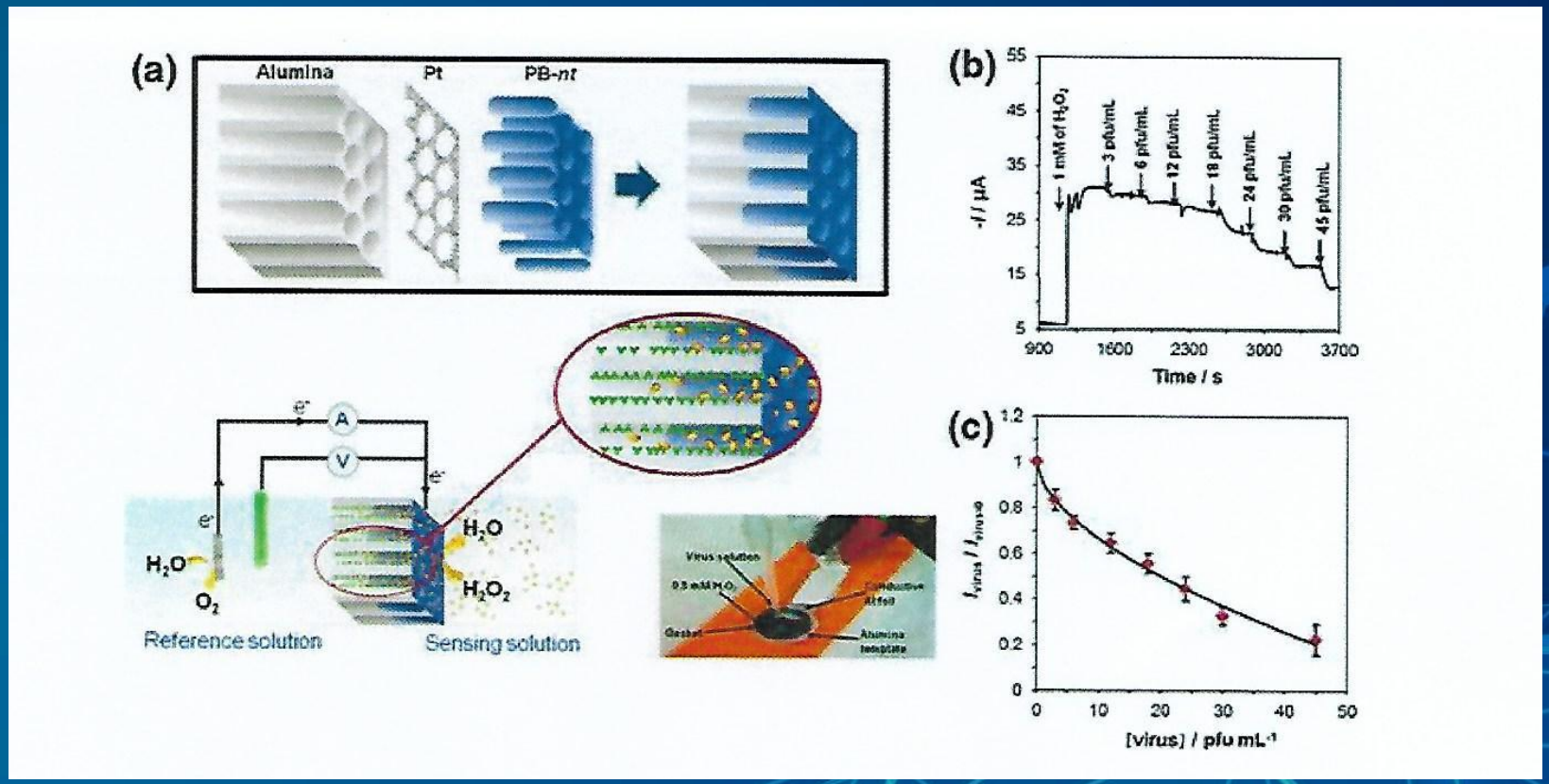

Fig. 15. (**a**) Schematic describing process of depositing Prussian blue nanotubes inside NAA pore and their use for virus sensing. (**b**) Typical closed- circuit steady-state current response of a PB nt based sensor toward DENV-2 virus and (**c**) its corresponding calibration plot showing normalized closed-circuit steady-state current versus virus concentration

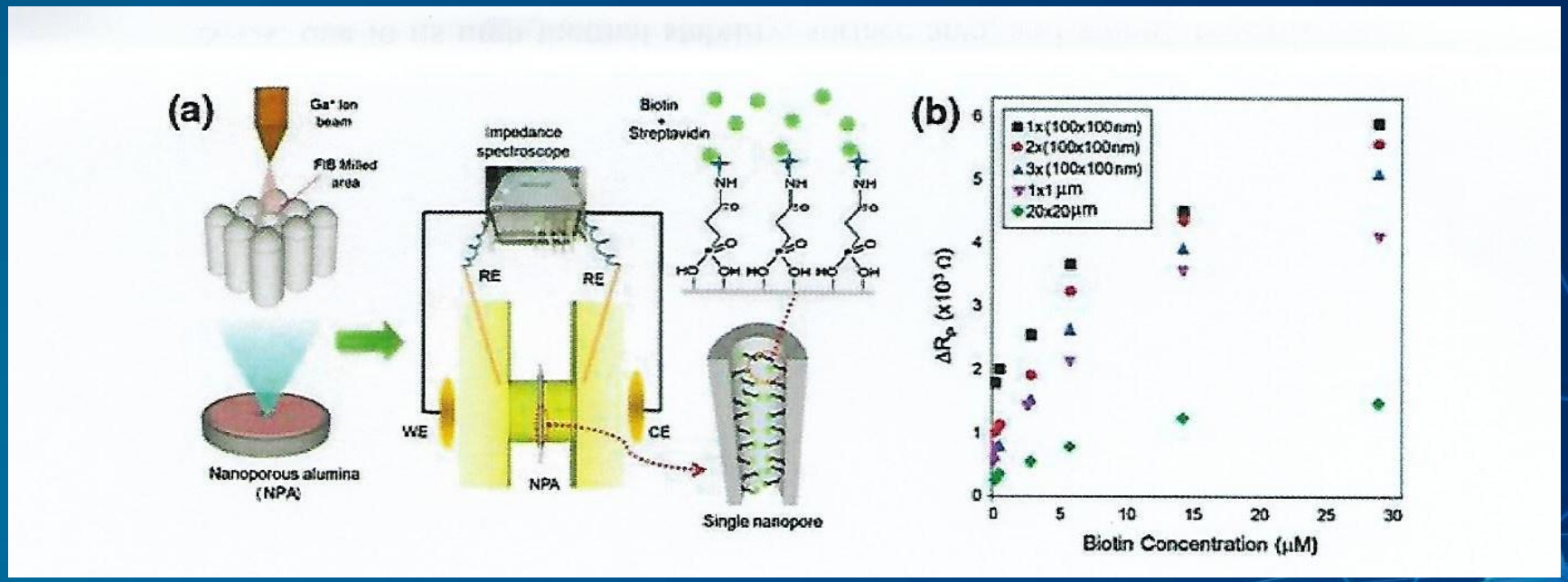

Fig. 16. (**a**) Schematic of NAA based impedance sensors for recognition of streptavidin and biotin interaction with selective area of pores opened with FIB and (**b**) graph showing changes of the pore resistance against various concentration of biotin for areas of pore opened using FIB.

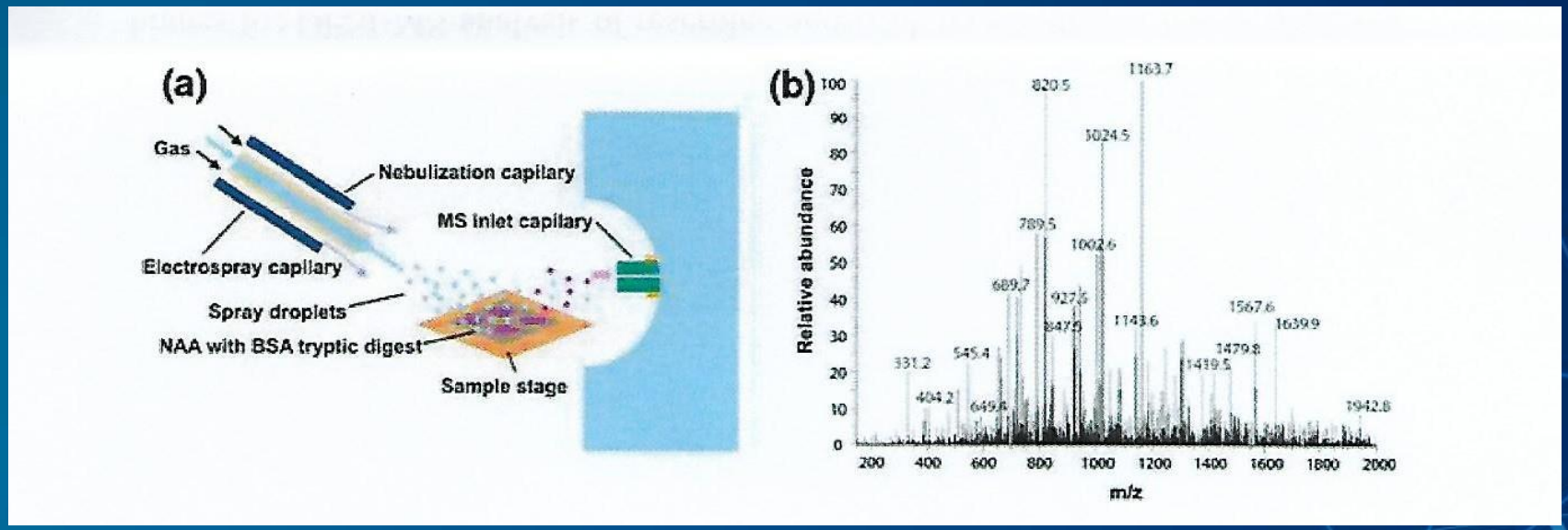

Fig. 17. (**a**) Schematic of the DESI MS experimental setup as describe by Knapp's group and (**b**) DESI MS mass spectrum of BSA tryptic digests on nanoporous alumina surface.

SUMARY

- Over the past several years, significant progress, has been made, with regards to structural engineering and surface modification of nanoporous AAO material. Much of this progress has been application-driven. In this review ,we have drawn together innovative approaches on controlling and designing structural growth of AAO with different sizes, arrangements, structures ,geometries and pores architectures.

- Access to these structures is achieved by changing anodization conditions such as current ,voltage and type of electrolytes during electrochemically self ordering of AAO.

SUMARY

- Researches are also pushing the boundaries of molecular separations using AAO with pores of controlled shape and size, internal surface modification and explore the effect external parameters, such as, pH, flux concentration gradient and ionic strength .

- An excellent consistency between experimental results and theoretical predictions of the interpore distance was observed for the highest studied anodizing time and the highest ethanol content in the anodizing electrolyte.

CONCLUSIONS

- Future reports on structural and chemical modifications of NAA will facilitate the development pf even smarter and advanced sensing devices
- Fabricated rugate filters based on NAA using a pseudo-sinusoidal anodization profile, which results in a continues gradient in effective refractive index of the layer
- Four different types of NAA rugate filters (NAA – RF) were prepared varying the anodization parameters and most sensitive NAA-RF was selected by studying the shift in stop band peak

CONCLUSIONS

- Applications for this nanostructured material for biomedical-separation-sensing and electronics
- Schematic of a pore of AAO membrane modified by adsorption on two polyelectrolytes pf opposing charge
- Schematic of a pore of AAO membrane modified by adsorption of two polyelectrolytes of opposing charge
- Schematic of electrically-responsive electro-polymer-coated AAO membrane showing reversible change of pore size between oxidation and reduction states

THANK YOU VERY MUCH FOR YOUR ATTENTION

* Prof Xavier Albort Ventura
* Tef 34-639-721-065
* Email: xavieralbort@ono.com